ELSEVIER

Hearing Research 130 (1999) 42–61

HEARING RESEARCH

Origins of medial geniculate body projections to physiologically defined zones of rat primary auditory cortex

Jeffery A. Winer [a,*], Sharon L. Sally [b], David T. Larue [a], Jack B. Kelly [b]

[a] *Division of Neurobiology, Department of Molecular and Cell Biology, University of California at Berkeley, Berkeley, CA 94720-3200, USA*
[b] *Laboratory of Sensory Neuroscience, Carleton University, Ottawa, Ont. K1S 5B6, Canada*

Received 26 March 1998; received in revised form 3 November 1998; accepted 8 November 1998

Abstract

Medial geniculate body neurons projecting to physiologically identified subregions of rat primary auditory cortex (area 41, Te1) were labeled with horseradish peroxidase in adult rats. The goals were to determine the type(s) of projection neuron and the spatial arrangement of these cells with respect to thalamic subdivisions. Maps of best frequency were made with single neuron or unit cluster extracellular recording at depths of 500–800 μm, which correspond to layers III–IV in Nissl preparations. Tracer injections were made in different cortical isofrequency regions (2, 11, 22, or 38 kHz, respectively). Labeled neurons were plotted on representative sections upon which the architectonic subdivisions were drawn independently. Most of the cells of origin lay in the ventral division in every experiment. Injections at low frequencies labeled bands of neurons laterally in the ventral division; progressively more rostral deposits at higher frequencies labeled bands or clusters more medially in the ventral division, and through most of its caudo-rostral extent. Medial division labeling was variable. Labeled cells were always in the lateral half of the nucleus and were often scattered. There were few labeled cells in the dorsal division. Seven types of thalamocortical neuron were identified: ventral division cells had a tufted branching pattern, while medial division neurons have heterogeneous shapes and sizes and were larger. Dorsal division neurons had a radiate branching pattern. The size range of labeled neurons spanned that of Nissl stained neuronal somata. Area 41 may receive two types of thalamic projection: ventral division input is strongly convergent, highly topographic, spatially focal, and restricted to one type of neuron only, while the medial division projection is more divergent, coarsely topographical, involves multiple cortical areas, and has several varieties of projection neuron. Despite species differences in local circuitry, many facets of thalamocortical organization are conserved in phylogeny.

Key words: Primary auditory cortex; Cerebral cortex; Auditory thalamus; Thalamocortical projection

1. Introduction

The auditory thalamus is responsible for integrating ascending streams of information and propagating these influences onto cortical (Romanski and LeDoux, 1993b [rat]) and subcortical (LeDoux et al., 1985 [rat]) structures. This task entails at least three processes. The first pertains to how thalamic principal cells and inter-

* Corresponding author. Tel.: +1 (510) 642-8227; Fax: +1 (510) 643-6791; E-mail: jawiner@socrates.berkeley.edu

Abbreviations: Aq, cerebral aqueduct; APt, anterior pretectum; BIC, brachium of the inferior colliculus; BV, blood vessel; CC, cerebral cortex; CG, central grey; CP, cerebral peduncle; CSC, commissure of the superior colliculus; D, dorsal nucleus or dorsal division; DD, deep dorsal nucleus; DS, dorsal superficial nucleus; Hip, hippocampus; HRP, horseradish peroxidase; IpN, interpeduncular nucleus; LGB, lateral geniculate body, dorsal nucleus; LGBd, lateral geniculate body, dorsal nucleus; LGBv, lateral geniculate body, ventral nucleus; LMN, lateral mesencephalic nucleus; LP, lateral posterior nucleus; LPc, lateral posterior nucleus, caudal part; LV, lateral ventricle; M, medial division; MGB, medial geniculate body; MB, mamillary body; MZ, marginal zone; NR, no response; Ov, pars ovoidea of the ventral division; PC, posterior commissure; Pt, pretectum; PL, posterior limitans nucleus; RN, red nucleus; SC, superior colliculus; Sg, suprageniculate nucleus; SN, substantia nigra; Spf, subparafascicular nucleus; SpN, suprapeduncular nucleus; Te1–3, see areas 41, 36, 20 below; V, pars lateralis of the ventral division; Vb, ventrobasal complex; wm, white matter; ZI, zona incerta; IIIv, third ventricle; 41, area 41/area Te1; 20, area 20/area Te2; 36, area 36/area Te3; Planes of section: C, caudal; R, rostral; V, ventral; M, medial; D, dorsal; L, lateral

0378-5955/99/$ – see front matter
PII: S0378-5955(98)00217-2

neurons perform their computational role in analyzing afferent signals (Hindmarsh and Rose, 1994). A second role is redistributive and involves many telencephalic cortical and subcortical structures which may be implicated in higher-order processing (Romanski and LeDoux, 1993a [rat]). Finally, corticofugal input to the thalamus could be decisive in gating subcortical sensory signals, providing descending control of neurotransmission (Diamond et al., 1992 [rat]), or in mediating other facets of receptive field organization (Sun et al., 1996 [bat]), to name just a few of the many possible dimensions (McCormick and von Krosigk, 1992 [guinea pig]).

The present study addresses the organization of thalamocortical neurons in the rat medial geniculate body and auditory cortex. Extracellular electrophysiological methods were used to identify frequency-specific cortical subregions, followed by tracer deposits within these regions and axoplasmic transport to label retrogradely the thalamic cells projecting to the auditory neocortex. We had four goals. First, we sought to identify all of the thalamic nuclei whose projections converge onto a subregion of auditory cortex as defined physiologically. Our second objective was to relate the types of relay neurons to their Golgi impregnated counterparts (Winer et al., 1999), and thus confirm whether there are varieties of thalamocortical neurons. This information would be useful for understanding parallels and differences among thalamic subdivisions and determining how many type(s) of neuron project to cortex. Third, these results support inferences about the arrangement of tonotopic representation in the nuclei of the auditory thalamus. Given the virtual absence of physiological studies of the thalamic distribution of best frequency in the rat (Kelly, 1990), the pattern of retrograde thalamic labeling might provide insight into the spatial topography of tonotopic representation. Finally, we wanted to obtain data that would form a natural basis for comparative studies in the cat and other species. This information might permit a more complete and balanced treatment of the principles of mammalian thalamocortical organization and encourage more explicit inferences about species differences.

2. Methods

All experimental and veterinary procedures were approved by the appropriate local institutional animal care and use committee. Electrophysiological mapping and connectional experiments were carried out in eight male Wistar albino rats (Charles River Laboratories, St. Constant, Québec), four of which provided the data for the subsequent anatomical analysis. For mapping, the rats were deeply anesthetized with Equithesin (3 ml/kg, i.p.), a mixture of chloral hydrate and pentobarbital sodium (see Sally and Kelly, 1988, for details [rat]). Areflexia was maintained for the several hours' duration of the experiment by supplemental injections of Equithesin (0.5 ml/kg, i.p., as required). The head was fixed in a customized holder that left the external meatus free. An incision was made in the scalp, the temporal muscle was retracted and a wide craniotomy exposed the lateral neocortex. The dura mater was removed and the surface of the cortex was coated with warm (37°C) dimethylpolysiloxane oil to prevent desiccation.

Multiple electrode penetrations were made into the auditory cortex to establish the pattern of tonotopic organization based on the frequency response of single neurons or the responses of small groups of neurons. Pargylene-insulated tungsten microelectrodes (1.3–2.1 MΩ) were inserted into the brain perpendicular to the cortical surface. Single unit action potentials and multiple spike recordings were recorded with a preamplifier (BAK model MDA-4) and window discriminator (BAK model DIS-1). Time locked action potentials were displayed as a poststimulus histogram on a signal averager (Tracor Northern). The responses were also displayed on an oscilloscope and monitored acoustically through a loudspeaker. A detailed drawing of the cortical surface representing blood vessels and surface landmarks served as a guide for subsequent microinjection of horseradish peroxidase (HRP) with regard to specific frequencies (see Sally and Kelly, 1988).

Physiological responses were evoked by 110 ms long tone pulses gated with 10 ms onset and offset times. Tones were presented through a high frequency tweeter (KEF model SP 1032) and a midrange loudspeaker (KEF model AD 5060) connected by a crossover network. The loudspeakers were mounted in a common enclosure 16 in from the animal's head and were aligned with the pinna axis (30° azimuth) in the sound field contralateral to the hemisphere from which recordings were made (usually the right hemisphere). The sound pressure level was calibrated by free field measurements with a 0.5 inch condenser microphone (Brüel and Kjaer type 4133) and a measuring amplifier. The sound system was capable of effectively delivering sounds from 500 Hz to 32 kHz with a roll-off in efficiency for higher and lower frequencies. The system was flat within ±6 dB between 2 and 38 kHz.

Best frequency (BF) was determined for each neuron or group of neurons by sweeping sound frequency across the rat's audible range at progressively lower sound pressure levels until the point of lowest threshold was determined. The BF was defined by the frequency that elicited a response at the lowest sound pressure level. Electrode penetrations were guided by our previous mapping experiments (Sally and Kelly, 1988) and were deliberately focused on a limited range of the frequency spectrum to avoid excessive damage to cortex or prolonged periods of deep anesthesia. Because

the purpose of the experiment required that the animals recover from the anesthetic, it was considered important to limit the duration of the recording session to 2–3 h rather than sampling many more neurons over much longer periods. Nevertheless, the samples included enough points to reveal a frequency gradient consistent with our findings in cases with much more extensive maps.

After a cortical region had been mapped for BF, the recording electrode was removed and replaced by a micropipette containing 30% HRP. The pipette tip was inserted into the auditory cortex and a small amount of enzyme was injected by pressure into a specific frequency region as defined by physiological mapping. The pipette was connected to a 1 μl Hamilton syringe by polyethylene tubing filled with distilled water. Injections were made slowly over a period of several minutes by a motorized drive connected to the Hamilton syringe. The volume of the injection was calibrated by movement of an air bubble along the length of tubing between the syringe and the micropipette. A typical injection was between 0.05 and 0.1 μl. Following an HRP injection the pipette was left in place for at least 5 min to allow for diffusion of the enzyme into the surrounding cortical tissue before being removed.

For connectional studies without physiological mapping, 30% HRP in sterile saline was pressure injected into auditory cortex through either a 1 μl Hamilton syringe or a glass micropipette (25 μm diameter tip) for smaller deposits. About 15 other experiments in which no physiological analysis was performed were available (Winer and Larue, 1987 [rat]). These large deposits were intended to define the borders of auditory cortex and to label extensive populations of cells in the medial geniculate body and posterior thalamus (Fig. 8A). In other experiments, more restricted injections were made within specific architectonic fields in auditory cortex (Fig. 8B).

Animals survived 2–3 days after injection. They were then anesthetized with pentobarbital sodium (60 mg/kg) and perfused through the heart with washout (physiological saline) followed by fixative (1% paraformaldehyde/1.5% glutaraldehyde in phosphate buffered saline [PBS]). The brains were removed and stored overnight in 30% sucrose/PBS. Frozen sections, 60 μm thick, were cut in the frontal plane and 3:4 were processed for HRP using tetramethylbenzidine as the chromogen (Mesulam, 1978). The remaining 1:4 series was processed with diaminobenzidine and counterstained with cresyl violet acetate to demonstrate cytoarchitecture and assess critically the boundaries of the deposit sites.

The measurements of Nissl stained or horseradish peroxidase labeled neural somata were made on experimental material. A total of 100 of each type of neuron were drawn with a 40× objective with a high numerical aperture and through a drawing tube. The somatic perimeters were smoothed to remove dendritic profiles and the areas were measured on a graphics tablet and computed using standard software (Sigma Scan™; Jandel Scientific, Sausalito, CA).

3. Results

3.1. Identification of the medial geniculate body

As a prelude to the integrated physiological-connectional experiments, we injected large amounts of either HRP or HRP conjugated to wheat germ agglutinin (WGA) to explore the thalamic boundaries of the medial geniculate complex. The injection itself (not shown) filled most or all of areas 41, 36, and 20 (Fig. 9A), and diffused into the rostral visual cortex as well. The temporal lobe regions involved correspond to primary and nonprimary auditory cortex as defined by architectonic criteria (Zilles et al., 1990; see also Burwell et al., 1995 [rat]). The ensuing mass of retrogradely labeled neurons extended from the extreme caudal tip of the auditory thalamus to its rostral pole (Winer et al., 1999, Figs. 9–12 [rat]). A section midway through the auditory thalamus showed the characteristic pattern in which each division had many retrogradely labeled neurons, while the adjoining, non-auditory nuclei had far fewer (Fig. 1). Even the medial division, whose thalamocortical projection is considered to be diffuse and divergent (Winer and Larue, 1987 [rat]), was filled with labeled neurons (Figs. 1 and 8A). In another experiment with a

→

Fig. 1. The labeled auditory thalamic neurons ensuing from a massive injection of horseradish peroxidase that included most of the auditory cortex. The pars ovoidea (Ov) in the ventral division provided a representative example showing how these divisions were established. Pars ovoidea neurons were smaller and more densely packed than those in the medial division (M). Cells in the subparafascicular nucleus (Spf) had a medial-to-lateral dendritic orientation, in contrast to the more vertical trend in the pars ovoidea. Deep dorsal nucleus (DD) neurons were smaller and had a pronounced stellate dendritic arrangement, and they were segregated by a fiber capsule from ventral division neurons. Finally, the pars lateralis (V) neurons had a much different fibrodendritic orientation: their long, gently curved rows contrasted with the complex organization in pars ovoidea. In conjunction with Nissl preparations and the other materials available (Winer et al., 1999), this permitted the secure delineation of even relatively small nuclei. The limits of the medial geniculate body were charted in an experiment in which several large injections of horseradish peroxidase in primary and nonprimary auditory cortex were made (see Fig. 9: left side). The retrograde labeling filled somata and dendrites sufficiently to allow the various neuronal types to be identified (Fig. 2) and the nuclear borders could be established and compared with those in other histological preparations (Winer et al., 1999, Figs. 1, 9–12 [rat]). Planapochromat, N.A. 0.65, ×312.

large injection, the thalamus was sectioned horizontally. The caudo-rostral extent of the medial division was ~1200 μm, a value in close correspondence with the estimates from cytoarchitectonic studies. Scattered neurons were labeled in the region between the rostral face of the medial geniculate body and unlabeled neurons in the ventrobasal complex (Fig. 8C); this area might correspond to parts of the posterior group of thalamic nuclei. Finally, in other experiments in which only the nonprimary auditory cortex was injected, the medial

geniculate body retrograde labeling was confined to dorsal division nuclei almost entirely (Fig. 8B).

3.2. Types of thalamocortical neuron

In the accompanying study of neuronal architecture, ten varieties of cells were identified in the three divisions of the medial geniculate body (Winer et al., 1999, Fig. 2 and Table 1 [rat]). Among the retrogradely labeled thalamic neurons in the present experiments, the dendrites were filled sufficiently in many specimens to allow the preliminary identification of some (if not the classification of all) of the types of cells projecting to auditory cortex. In the ventral division, the neurons had a bipolar or multipolar form resembling that of bushy tufted cells (Fig. 2E: 1). The dorsal nuclei contained many examples of tufted (Fig. 2D: 3) and radiate (Fig. 2A,C: 4) neurons interspersed. The medial division, whose neuronal architecture was the most diverse, had also the most varied population of retrogradely labeled neurons, including magnocellular (Fig. 2B: 6), wide field (Fig. 2B: 7), tufted spindle (Fig. 2B: 8), and horizontal (Fig. 2B: 9) neurons. While this classification rested primarily on the dendritic configuration of the retrogradely labeled neurons, factors such axosomatic size, shape and orientation produced additional evidence. No examples of smaller neurons corresponding to putative Golgi type II cells (Winer et al., 1999, Table 1, types 2, 5, 10) were seen, and the profiles of neurons with appreciable somatodendritic filling were readily related to their Golgi impregnated counterparts.

3.3. Thalamic projections to physiologically defined primary auditory cortex

In the first mapping and connectional experiment, four small tracer deposits were made in the caudodorsal part of area 41 (Fig. 3A: left side), as defined on the basis of its physiological organization (Fig. 3A: center) and its appearance in Nissl preparations (see Games and Winer, 1988, for architectonic details [rat]). The injections were targeted at $\sim$2 kHz, though the tracer diffused caudally (towards lower frequency regions in this field) as well as dorsally (into adjoining nonprimary cortex) above area 41 (Fig. 3A: center). It appears unlikely that extracellular tracer diffusion could have contributed materially to the pattern of thalamic labeling for three reasons. First, there were no retrogradely labeled somata in thalamic nonprimary visual nuclei (Fig. 3B–E), as would be expected if the spread were a significant factor in retrograde transport. Second, the individual injections never invaded the white matter (Fig. 3A: right side, wm); had they done so, thalamofugal axons passing more rostrally might have been interrupted, resulting in retrogradely filled neurons scattered through large expanses of the auditory thalamus. Third, the thalamic cells labeled by the injections were distributed predictably and topographically. This pattern was in close alignment with the results from other studies in which the locus of retrogradely labeled neurons could be related systematically to the site of injection (Deacon et al., 1983; Winer and Larue, 1987; Clerici and Coleman, 1990 [rat]). Subsequent experiments (Figs. 4–6) followed the same patterns with regard to injection sites, and those chosen as representative of the injection site in this and the following cases show the maximal extent of the individual deposits. All deposits do not appear in one section since they were not aligned perfectly with the blocking and sectioning plane.

In each experiment, four or five representative thalamic sections were chosen to illustrate the chief results; intervening sections had a comparable distribution and density of labeling. The main focus of retrograde labeling in this case was a band of neurons about 300 μm wide and 800 μm tall that filled much of the lateral quarter of the ventral division (Fig. 3C: V). There were virtually no labeled neurons in the medial division, a result that distinguished this experiment from the others. The few such cells in or near the medial division were at its border with the ventral division and could not be assigned to either division with confidence. The dorsal division likewise was virtually devoid of labeling (Fig. 3C: D). More rostrally, the ventral division neurons formed a circumscribed ring along the ventrolateral border with the dorsal division (Fig. 3D), with a few scattered neurons extending medially. The most rostral labeling was a continuation and subset of the band in the ventral division.

While it is valid to infer from this experiment (and the others) that a cortical volume is represented by a corresponding thalamic territory, sections limited to two planes provide little evidence about the three-dimensional organization of such a territory. To address this issue, we reconstructed the borders of the labeling and represented them as a polygon from transverse sections and projected these onto horizontal sections. The matching borders from Nissl stained sections (Fig. 7) are likewise aligned with the reconstruction and the architectonic subdivisions, and the results from the intervening sections were interpolated (not illustrated). The resulting projection shows that about one-third of the auditory thalamus was devoted to a comparatively modest cortical sector, particularly since the effective injection sites (Figs. 3–6: right inset, white regions) were usually $\sim$200 μm in diameter. This implies appreciable branching, and possible convergence, of thalamocortical afferents.

In a second experiment the injection sites were situated $\sim$300 μm rostrally within area 41; despite a 900 μm long trail of diffusion extending toward area 19 (Fig. 4A: left side), there was no retrograde labeling in the visual thalamus (Fig. 4D–F). There were three

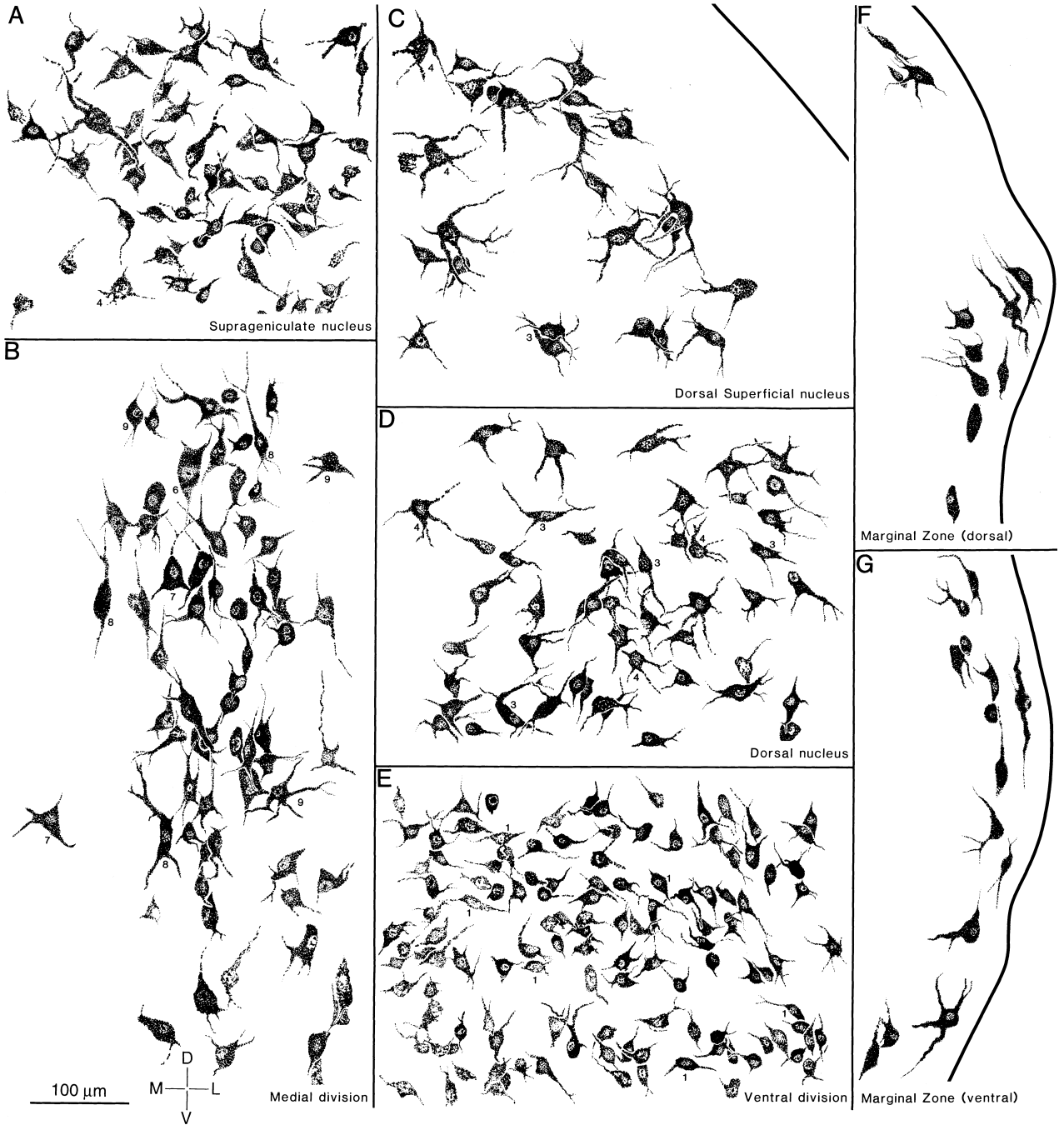

Fig. 2. Types of neurons retrogradely labeled in medial geniculate body subdivisions compared with their presumptive counterparts as seen in Golgi preparations (Winer et al., 1999, Figs. 2–5). A: Suprageniculate nucleus neurons were large multipolar cells (4) with radiating dendrites (for details, see Winer et al., 1999: Table 1). They were more clustered than nearby cells in the dorsal superficial nucleus (C) and smaller than those in the medial division (B). Protocol for all panels: Planachromat, N.A. 0.65, ×500. B: Medial division neurons were unusual for their heterogeneous shapes and sizes and the wide range of their orientations. The varieties labeled included magnocellular (6), wide field (7), tufted spindle (8) and horizontal (9) neurons. A more detailed analysis of the features distinguishing them is available (Winer et al., 1999). These neurons were distinct from suprageniculate neurons (A) because of their more vertical orientation. Their variety set them apart from dorsal superficial nucleus cells (C) and from neurons in the dorsal nucleus (D), both of which were more clearly stellate or radiate, and from ventral division neurons (E), whose dendritic arrangement was orthogonal to that of medial division cells. Marginal zone neurons (F, G) were sparse and had a far more vertical orientation. C: Dorsal superficial nucleus neurons corresponded closely to the profiles of two of the three cell types defined in Golgi preparations (Winer et al., 1999, Figs. 1, 4). Tufted neurons (3) were strongly oriented along the medio-lateral axis and their dendrites arose at the somatic poles, while radiate cell (4) primary dendrites arose from the somatic perimeter without any preference. D: Both tufted (3) and radiate (4) neurons were labeled in the dorsal nucleus (D). E: In the ventral division (V) only tufted neurons were labeled retrogradely, and they formed clearly oriented laminae. F, G: The affiliations of the marginal zone, both functional and anatomical, are obscure (see Winer and Morest, 1983b, 1984 [cat]). The retrogradely labeled neurons were unexpectedly numerous, appear to be predominantly tufted, and were larger than those in the ventral division (E).

important differences between this and the first experiment. First, the labeling in the ventral division was far more clustered rostrally than it was in more caudal sections. Second, there were a few cells in the dorsal division, which was unexpected, since the injection was remote from the fields that are thought to be dorsal division targets (Winer and Larue, 1987; Arnault and Roger, 1990 [rat]). Third, the medial division had an appreciable number of labeled neurons.

As might be expected from the first experiment (Fig. 3C), a band of retrogradely labeled neurons was present in the ventral division (Fig. 4E) after cortical deposits centered at 11–12 kHz (Fig. 4A: center inset). This suggests that progressively more anterior injections will be represented at successively more medial foci in the ventral division. While this is correct as a first approximation, it cannot explain the complete distribution of ventral division neurons in this experiment. For example, there are a few labeled neurons near the border of the ventral and medial divisions (Fig. 4C), which would correspond to the putative high frequency representation and therefore violate a strict tonotopic/topographic principle as described above. Alternatively, the injection might have encroached slightly into the white matter (Fig. 4A: right side). The counterargument to the transected fibers interpretation is the possibility that the 2 kHz injections, which never entered the white matter (Fig. 3A: right side), nevertheless labeled some cells in the medial part of the ventral division (Fig. 3C: V), whereas the 22 kHz experiment (Fig. 5A) had an unexpectedly wide thalamic representation (Fig. 5: black inset) that appeared to violate an absolute thalamic lamina-to-cortical column transformation implicit in a simple topographic model. These issues will be examined further in Section 4.

A few neurons in the dorsal nucleus were labeled (Fig. 4C: D), as in the 2 kHz experiment (Fig. 3C: D). As noted above, we considered these as evidence of involvement of extra-auditory cortex (Fig. 3A, Fig. 4A: left side and center). However, a similar small cluster was found in the 22 kHz case (Fig. 5B), whose injections were confined entirely to area 41 (Fig. 5A: center). Interestingly, the 38 kHz deposits (Fig. 6A: center), which also were confined to area 41, had no labeled dorsal division neurons (but see Fig. 6D).

The labeling in the medial division (Fig. 4B–E) was surprisingly heavy, in contrast to the first (2 kHz) experiment (Fig. 3B–E), in which there was essentially no medial division projection. There was no regular spatial distribution of the labeling within the medial division. In some sections it was in the central part of the medial division (Fig. 4B: M), in others it lay in the ventralmost part (Fig. 4D: M) or it was scattered (Fig. 4E: M) or sometimes absent (Fig. 4F: M). Considered across experiments, the medial division had the most variable distribution, while the ventral division had the most predictable pattern; in the dorsal division, so few neurons were labeled that no certain conclusions about its projection to area 41 were possible.

The global regions of retrograde labeling (Fig. 4: black inset) in the medial (M) and ventral (V) divisions largely overlap in the caudo-rostral axis. This had two interesting implications for the frequency-specific organization within the medial geniculate body. First, it suggests a basic difference between the ventral and the medial divisions: in the former, this arrangement was evident in every experiment, and it is consistent with the interpretation that best frequency has a caudal-to-rostral representation whose structural counterpart is fibrodendritic lamination. Second, the amount of retrograde labeling in the medial division was far more variable, ranging from no cells (Fig. 3: M) to a few neurons (Fig. 6A: M) or to many (Fig. 4B: M, Fig. 5C: M).

→

Fig. 3. Results from injections at 2 kHz. A: Lateral views (left side) show the location of primary auditory cortex (area 41; light stippling) projected onto the hemisphere, with the accompanying injection sites (black dots) and the zone of tracer diffusion (dark stippling). A more detailed reconstruction (center) with the physiological recording sites (dots) and best frequencies (numbers) superimposed upon the blood vessels (fine lines). The architectonic boundaries of area 41 were determined independently from Nissl preparations, as were those of the medial geniculate body subdivisions (see below). View (right side) of the largest of the four injections in a transverse section through the center of the track (thin black line), the estimated effective site of the injection (white perimeter), and the diffusion; the latter region was not considered to have contributed to thalamic retrograde labeling. B–E: Caudal-to-rostral sequence of representative sections that demonstrated the auditory thalamic input to the 2 kHz region; each dot corresponds to one labeled neuron. Black inset, horizontal reconstruction in which the perimeter demarcating the retrogradely labeled neurons was drawn as a convex polygon (stippled); this represented a two-dimensional reconstruction of the medio-lateral and caudo-rostral distribution of thalamic labeling. The thin black horizontal lines (arrowheads) match the transverse position of the sections in panels B–E. B: A few labeled neurons lay along the medial wall of the central division (V), in the presumptive high-frequency sector (see Fig. 6D: V). C: Labeling was concentrated in the lateral one-quarter of the ventral division, in the pars lateralis. Smaller clusters of labeling persisted medially, however, and a new focus occurred ventromedially. These foci lay medially in this section, suggesting that the analogous neurons in the preceding section (B) were properly included in the ventral, and not in the medial, division. In this and the following experiments (Figs. 4–6), all the medial division transport was confined to the lateral one-half. If there is any systematic representation of best frequency, then more than $\sim$4 octaves are compressed in a medio-lateral span of $\sim$300 μm, while the medial one-half would represent frequencies $>$38 kHz. D: This section contained the most focal concentration of labeled neurons. The gaps at the inferior part of the column may reflect that the injections were concentrated in the uppermost half of the 2 kHz representation. E. The labeling pattern here was consistent with the view that isofrequency representations are arranged dorso-ventrally in the ventral division (see Fig. 9 and Section 4).

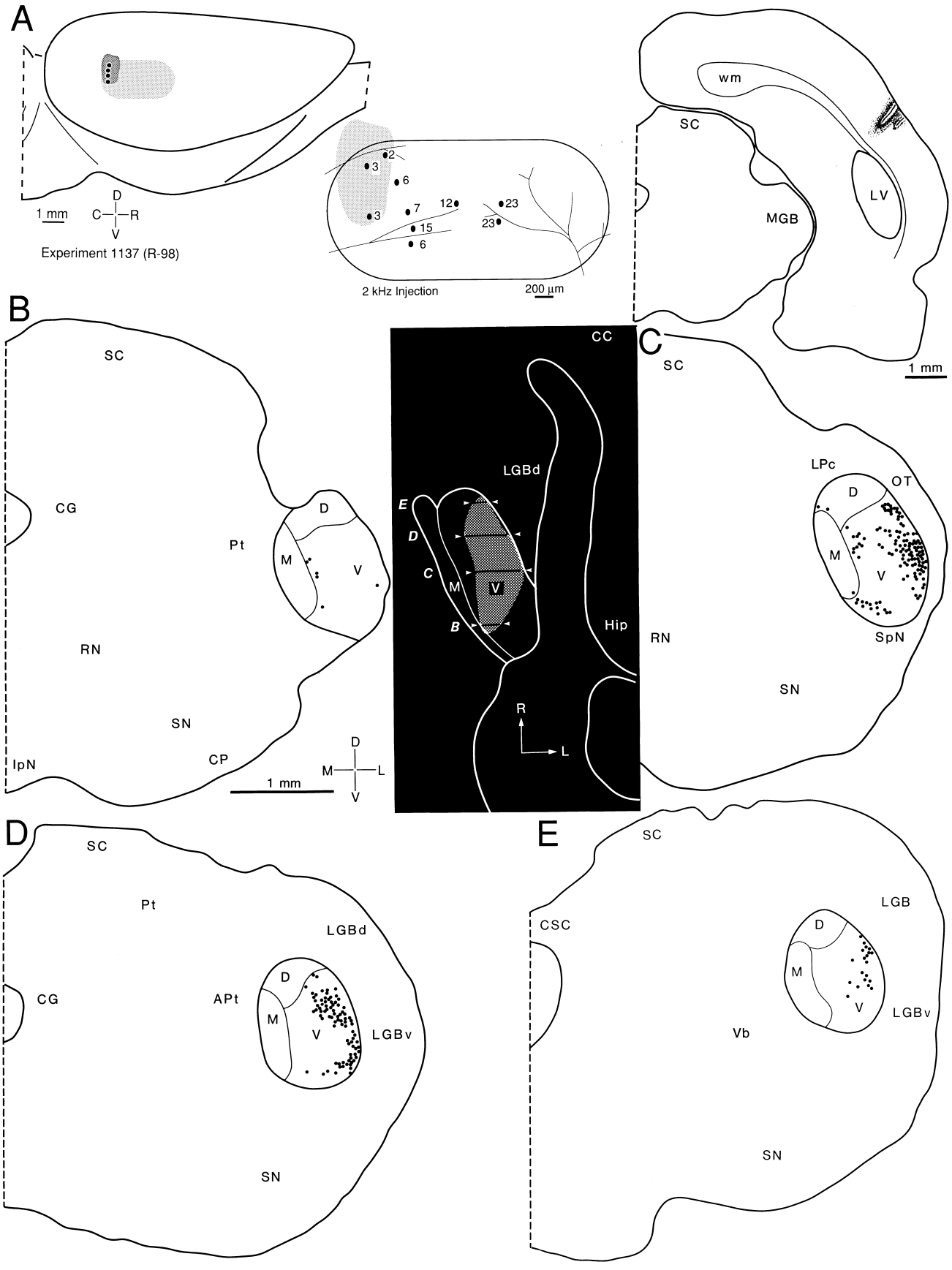
A
1 mm
D
C
R
V
Experiment 1137 (R-98)
2
3
6
3
7
12
23
23
15
6
2 kHz Injection
200 μm
wm
SC
LV
MGB
B
SC
CG
Pt
D
M
V
RN
SN
IpN
CP
1 mm
D
M
L
V
CC
LGBd
E
D
C
M
V
B
Hip
R
L
C
SC
1 mm
LPc
OT
D
M
V
SpN
RN
SN
D
SC
Pt
LGBd
CG
APt
D
M
V
LGBv
SN
E
SC
CSC
LGB
D
M
V
LGBv
Vb
SN

The next experiment studied the projections to the 22 kHz cortical representation (Fig. 5). The usual row of four deposits was made; diffusion may have involved some frequencies remote from 12–22 kHz (Fig. 5A: center). The deposits did not enter the white matter (Fig. 5A: right side), and the area of the injections was approximately the same as in the prior experiments, suggesting that its projections might be area-specific.

Three features distinguished this experiment. The ventral division labeling was the most diffuse seen in any of the cases. There were a few neurons labeled in the dorsal division. Finally, the medial division projection arose almost entirely from the caudal half of the auditory thalamus.

The most unexpected result was the broad distribution of retrograde labeling in the ventral division (Fig. 5C: V), which encompassed most of its medio-lateral axis (Fig. 5: black inset). An equally surprising finding was that the most rostral focus of labeling was more lateral in the ventral division (Fig. 5D: V) than would have been predicted on the basis of the 2 kHz (Fig. 3D: V) or 11–12 kHz (Fig. 4D: V) deposits. The lateralmost transport cannot be attributed to severing axons in the white matter, since the low frequency (<12 kHz) region is caudal to this, and because tracer diffusion alone is unlikely to produce significant retrograde labeling.

The sparse labeling in the dorsal division (Fig. 5B) may represent a small projection since the injections, including their diffusion, were confined to area 41. Dorsal division involvement was limited to the caudal two-thirds of the medial geniculate body.

The projection of the medial division was restricted essentially to the caudal half of the auditory thalamus (Fig. 5: black inset). However, this experiment labeled by far the largest number of medial division neurons in any experiment, and they formed a conspicuous band near the border with the ventral division. These neurons were clustered in a sharply defined region 200 μm wide and 500 μm high; there were few neurons labeled more medially.

The final experiment differed from its predecessors in several ways (Fig. 6). As expected, the ventral division labeling formed a discrete band; however, the configuration of the mass of labeled cells was highly variable along the caudo-rostral axis. A second finding was that no dorsal division neurons were involved in this projection. Finally, only the most caudal part of the medial division had any labeled neurons.

The four deposits were confined to area 41 and they were targeted at $\sim$38 kHz. The injections formed their usual columns $\sim$300 μm wide, and their orientation was inclined slightly (Fig. 6A: right side) from the almost perpendicular registration in the preceding experiments (Fig. 3A, Fig. 4A, Fig. 5A: right side). The shape of the ensemble of labeled neurons was remarkably varied in the caudo-rostral axis, ranging from a horizontally arranged sheet 500 μm wide by $\sim$100 μm thick at the caudal part (Fig. 6C: V) to a more oblate configuration in the pars ovoidea more rostrally (Fig. 6D: at the border of M and V). The labeling ended as a vertically arranged group of cells in the most lateral and anterior part of the pars lateralis. This implies that an isofrequency lamina, insofar as it can be represented by such injections, has a complex, three-dimensional spatial geometry that cannot be represented as a simple linear projection of thalamic axons onto the cerebral cortex.

Medial division projections, in contrast, were limited to a few neurons concentrated in the most caudal part of the auditory thalamus (Fig. 6B: M). Lower frequency (2 kHz; Fig. 3) deposits produced little such labeling, while middle (11–12 kHz; Fig. 4) and higher (22 kHz; Fig. 5) frequency injections labeled many more neurons at several medial division loci.

4. Discussion

Placing the present results within a functional context entails both practical and conceptual problems. The practical constraint is that the limited amount of physiological work presently available on the rat medial geniculate body makes it difficult to summarize the rules governing tonotopic, binaural, or other forms of

→

Fig. 4. Results from 11–12 kHz injections; for details of format, see the legend to Fig. 3. A: While the injections were centered in area 41, there was appreciable diffusion into caudodorsal Te2D?/Oc2L (nomenclature after Zilles et al., 1990). The ensuing pattern of retrograde transport (panels B–F) suggests that the diffusion did not confound the experiment, since there was no labeling in the visual thalamus, and because the auditory thalamic transport was consistent with that in other experiments (Figs. 3, 5 and 6). The black inset shows the independence of the foci of labeling in the ventral (V) and medial (M) divisions, and their antero-posterior discontinuity, and their congruence medio-laterally. B: This was the most caudal section in these experiments with appreciable medial division labeling. C: The dorsal division labeling was significant only in this section and in a few others (Fig. 5B,D). With regard to the dorsal and ventral divisions, this suggests strong nucleus-to-area affiliations. D: The medial division had a characteristic distribution of neurons in the lateralmost half, while the ventral division labeling was unexpectedly broad along the medio-lateral dimension. E: This distribution resembled that in the preceding, 2 kHz, experiment (Fig. 3D,E: V), and it supports a relation predicted between a thalamic lamina and a cortical isofrequency contour (Fig. 9). F: A few neurons near the rostral pole of the auditory thalamus lay far more laterally than expected, and thus violated the simple prediction of a lamina-to-a-contour relationship, or perhaps represented a shift toward higher frequencies more rostrally.

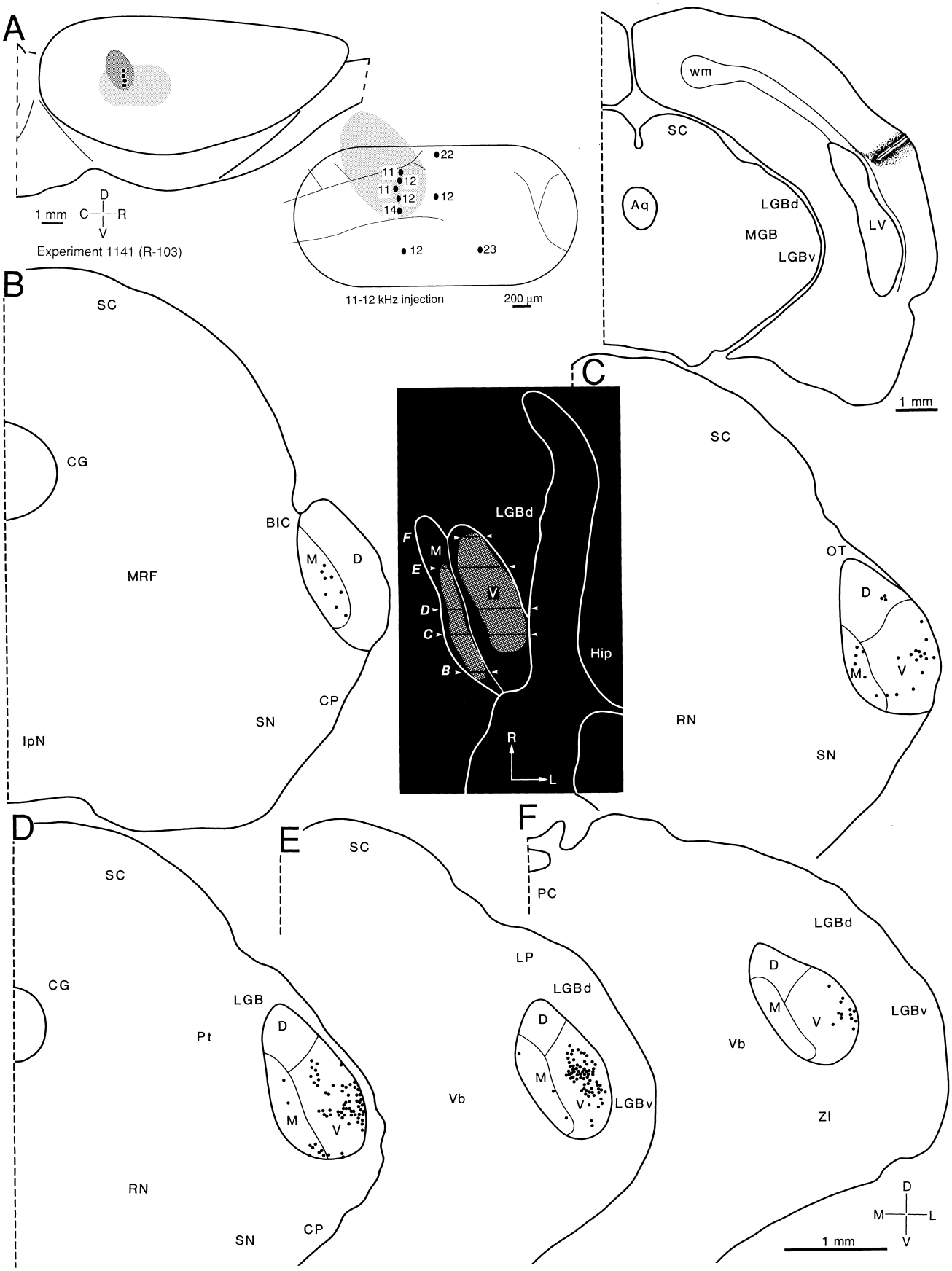
A
D
1 mm C R
V
Experiment 1141 (R-103)
22
11 12
11 12
12 12
14
12
23
11-12 kHz injection
200 μm
wm
SC
Aq
LGBd
MGB
LGBv
LV
1 mm
B
SC
CG
BIC
MRF
M
D
SN
CP
IpN
C
LGBd
F
M
E
V
D
C
B
Hip
R
L
SC
OT
D
M
V
RN
SN
D
SC
CG
LGB
D
Pt
M
V
RN
SN
CP
E
SC
LP
LGBd
D
M
V
LGBv
Vb
F
PC
LGBd
D
M
V
LGBv
Vb
ZI
D
M L
V
1 mm

organization. It might be argued that this issue is not critical since a considerable body of data is available in the cat (Clarey et al., 1992), and that the basic principles in the feline auditory thalamus ought to be extended to the rat, at least provisionally. However, there is evidence of fundamental interspecific differences in medial geniculate body organization. For example, there are few GABAergic neurons in the rat auditory thalamus ($<1\%$; Winer and Larue, 1988, 1996), and many more in other species ($>25\%$; Smith et al., 1987 [monkey]; Winer and Larue, 1996 [cat, monkey]). This implies that some as yet unspecified, GABA-dependent processing is expressed robustly in the cat, while in the rat such processing must be attenuated or organized along fundamentally different principles. A second, conceptual consideration is ecological, and may be related to species specific differences in circuitry. Cats are nocturnal predators adept at localizing and tracking their prey in acoustically challenging environments, while rats scavenge and avoid detection by stealth. It would seem implausible to regard the rat medial geniculate body simply as a miniaturized version of the cat's, in terms of either size or function. By the same token, more than 10 feline cortical auditory areas have been distinguished (Aitkin, 1990), while in the rat only a few such regions have been identified (Kelly, 1990; Burwell et al., 1995). If such differences are genuine, then their implications for the thalamus remain to be articulated.

4.1. Thalamic projections to cortex

To what degree can the present findings in the rat be generalized to other species? At least for area 41/Te1, two auditory thalamic nuclei – the ventral and the medial divisions – are the primary sources of input, a pattern much like that in the cat with regard to primary auditory cortex (AI) (Niimi and Naito, 1974). A second parallel is the common structure of thalamocortical neurons in both the ventral division and the medial division in the rat and cat (Table 1). The cat ventral division contains bushy tufted principal cells (Morest, 1964) that project to AI (and to its more rostral partner, the anterior auditory field), while rat ventral division neurons have a comparable structure (Clerici et al., 1990; Winer et al., 1999) and an analogous projection (Clerici and Coleman, 1990) with regard to area 41/Te1. A further correspondence is that the laminar target of the ventral division is chiefly in layers III and IV (Vaughan, 1983 [rat]; Sousa-Pinto, 1973 [cat]; Jones and Burton, 1976 [monkey]; Hashikawa et al., 1995 [monkey]). The concordance among these different dimensions is strong circumstantial evidence that common patterns of organization can be derived, at least to a first approximation, for this segment of the auditory forebrain. Much the same argument can be made with regard to the neuronal structure of the medial division (Winer and Morest, 1983a [cat]; Winer et al., 1999 [rat]) and with respect to its ascending projections (Niimi and Naito, 1974 [cat]; Ryugo and Killackey, 1974 [rat]). Such parallels cannot be extended to every aspect of auditory thalamic organization since (as noted above) there are substantial qualitative and quantitative species differences in the proportion of GABAergic neurons.

4.2. Representation in the isofrequency domain

The systematic representation of best frequency is a cardinal feature of auditory cortical organization (Schreiner, 1992) and, by extension, in the corresponding thalamic nuclei as well. In other species, the relation between the fine-grained tonotopic map in the ventral division (Imig and Morel, 1985 [cat]) and the corresponding representation in auditory cortex (Reale and Imig, 1980 [cat]) is relatively well established (Middlebrooks and Zook, 1983 [cat]). The structural basis for the ordered map of frequency is believed to be the fibrodendritic laminae, which consist of principal tufted cell dendritic arbors and the terminal plexus of afferent

→

Fig. 5. Results from 22 kHz injections. A: The four deposits were restricted to area 41 (left side). The physiological range of best frequency spanned ~12–25 kHz (center), with the injections centered in the 18–22 kHz region. The sparse white matter labeling below the deposit was transport, not diffusion; the dorsal disposition of these axons suggests possible commissural labeling. This experiment had the most widely distributed labeling in our series (compare with Figs. 3, 4 and 6), involving most of the caudo-rostral, and much of the medio-lateral, axes of the ventral division (black inset). The medial division labeling was concentrated caudally and laterally, as in the other experiments. B: The labeling involved, to varying degrees, each of the three primary divisions. Most labeled neurons in each division were near the lateral or ventral nuclear border. C: Since the deposit filled only ~20% of area 41 (panel A, center), the retrograde transport occupied a disproportionately large part of the ventral division (V), and suggested considerable thalamocortical convergence. Indirect evidence that the isofrequency plane's main axis was dorso-ventral comes from the label-free ventral division subregions above and below the foci of transport. In contrast, injections that crossed a cortical architectonic border (Fig. 3A: center) labeled cells that extended to the thalamic border in at least some sections (Fig. 3D: V). D: A progressive, caudal-to-rostral decline of medial (M) and dorsal (D) division labeling occurred. Ventral division projection neurons were concentrated predominantly in the pars lateralis (see also panel C). This suggests that frequencies <22 kHz were underrepresented spatially, or that there was an antero-posterior (as well as a dorso-ventral) counterpart to the representation of best frequency; these possibilities are not mutually exclusive. E: Near the rostral pole, ventral division neurons were more central than those in more caudal sections (panels C, D), consistent with the dorso-ventral hypothesis of representation. Here as well, the label-free zones above and below the focus were in accord with the dorsal and ventral, uninjected regions above and below the deposits (panel A, center).

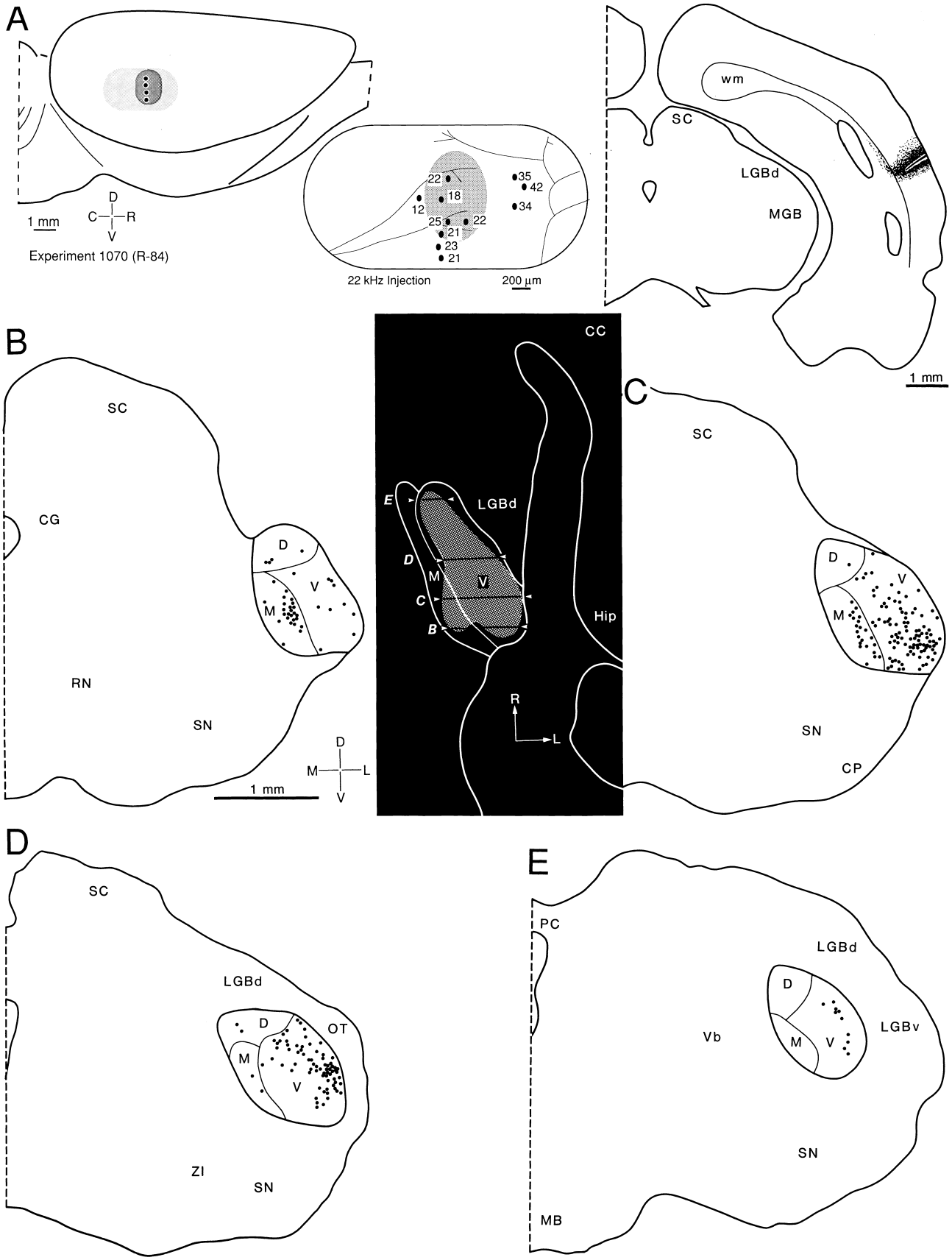
A
1 mm
D
C
R
V
Experiment 1070 (R-84)
22
18
12
25
22
21
23
21
35
42
34
22 kHz Injection
200 μm
wm
SC
LGBd
MGB
1 mm
B
SC
CG
D
V
M
RN
SN
1 mm
D
M
L
V
CC
E
LGBd
D
M
V
C
B
Hip
R
L
C
SC
D
V
M
SN
CP
D
SC
LGBd
D
OT
M
V
ZI
SN
E
PC
LGBd
D
Vb
M
V
LGBv
SN
MB

Table 1
Comparison of primary and nonprimary streams in the ventral and medial divisions of the auditory thalamus

Dimension	Ventral division	Reference	Medial division	Reference
Modality specificity	Auditory	Aitkin and Webster (1972)	Polysensory	Wepsic (1966)
Tonotopic organization	Precise	Imig and Morel (1985)	Coarse	Rouiller et al. (1989)
Tuning curves	Sharp	Calford and Webster (1981)	Broad	Calford (1983)
Multimodal integration	None	Clarey et al. (1992)	Prominent	Aitkin (1973)
Cortical projection	Convergent	Brandner and Redies (1990)	Divergent	Huang and Winer (1997)
Laminar cortical target	Layers III, IV	Vaughan (1983)[a]	Layers I, VI	Ryugo and Killackey (1974)[a]
Subcortical target(s)	Thalamic reticular nucleus[b]	Harris (1987)[a]	Amygdala and striatum	Shinonaga et al. (1994)
Probable transmitter	Glutamate	Popowits et al. (1988)[a]	Glutamate	LeDoux and Farb (1991)[a]
Topography of projection	Focal	Patterson (1976)[a]	Diffuse	Arnault and Roger (1990)[a]
Type(s) of neuron	Two	Winer et al. (1999)[a]	Five	Winer et al. (1999)[a]
Type(s) of thalamocortical neuron	One	Present study[a]	Four	Present study[a]
Type(s) of GABAergic neuron	One	Winer and Larue (1988)[a]	One (?)[c]	Winer and Larue (1988)[a]
Physiological plasticity	Limited	Weinberger and Diamond (1987)	Robust	Gerren and Weinberger (1983)
Effects of lesioning	None or modest	Kelly and Judge (1985)[a,d]	Integrative deficit	Glassman et al. (1975)[e]

[a]Rat; unmarked citations refer to cat.
[b]In the rat ventrobasal complex.
[c]A range of sizes was seen in a small sample of immunopositive neurons.
[d]Bilateral lesions.
[e]Unilateral lesions.

axons of midbrain origin, both of which are polarized and form fibrodendritic laminae oriented dorso-ventrally (Morest, 1964, 1965 [cat]). While the frequency representation must be continuous, each lamina is believed to constitute a more or less discrete sector with a periodicity of ~50 μm/lamina; this estimate is based primarily on neurons in the pars lateralis and it suggests that there is a topographic pattern of thalamocortical projection in the rat which resembles the arrangement in the cat, at least to a first approximation. Four features constrain any more refined estimate of tonotopy in the rat. The first is that the dendritic arbors of principal tufted neurons are often much wider than those of similar neurons in the cat, up to 80 μm. Since a range of about eight octaves is represented physiologically across the ~3500 μm caudo-rostral span of area 41, this yields a value of approximately 450 μm/octave, assuming a linear thalamic-place to cortical-areal projection for an isofrequency contour. However, high best frequencies may be overrepresented (Sally and Kelly, 1988). A second limitation is that the ventral division itself is never more than ~800 μm wide, and often much narrower. If the thalamic representation preserves the ratio of frequency-to-area found in primary cortex, then a value of 100 μm/octave might approximate the case. This could account for the apparent overrepresentation from deposits that are limited to ~1 octave in the cortex, yet span more than half the width of the ventral division (Fig. 5C).

A third issue that could distort the frequency-specific representation in the rat ventral division is the paucity of Golgi type II neurons (Winer and Larue, 1988). Their axons and dendrites are, in the cat, important contributors to the laminar fibrodendritic plexus (Mor-

→

Fig. 6. Results from a 38 kHz injection. A: Each deposit was limited to area 41 (left side) and probably included frequencies from ~36–40 kHz (center). The deposit shown did not reach the white matter (right side) and was slightly oblique to the cortical surface. The retrograde labeling (black inset) extended from the posterior one-third of the ventral division (V) to its anterior extremity, with minimal involvement of the medial division (M) except caudally, where the lateral half of the nucleus was labeled. B: The heaviest concentration of medial division labeling was slightly rostral to that from the 11 kHz injection (Fig. 4B: M) and caudal to that from 22 kHz (Fig. 5B: M) deposits, suggesting that any topographic cortical projection was irregular or complex. C: In the pars ovoidea, a thin sheet of retrogradely labeled neurons was oriented medio-laterally. The transport defined almost exactly the border between the ventral and medial divisions, suggesting that still higher frequencies are displaced ventromedially within the dorsal division. D: As the laminae in panel C extended rostrally, they began to turn, and the neurons formed a more circular cluster that extended dorsally in more anterior sections. A few labeled cells lay in the medial division and along the dorso-lateral perimeter of the dorsal division. E: The retrogradely labeled neurons in the rostral pole were far lateral to those from the 22 kHz injection at the matching thalamic level (Fig. 5E). This implies, at least for higher frequencies, there is not a simple thalamic-laminar to cortical-isofrequency contour transformation. The horizontal sheet of neurons (panel C) and the cluster (panel D) have now rotated 90° to form a vertical ensemble. The dorsal and central extremities of this column were devoid of labeling, and the injection (panel A, center) was far from the dorsal and ventral borders of area 41.

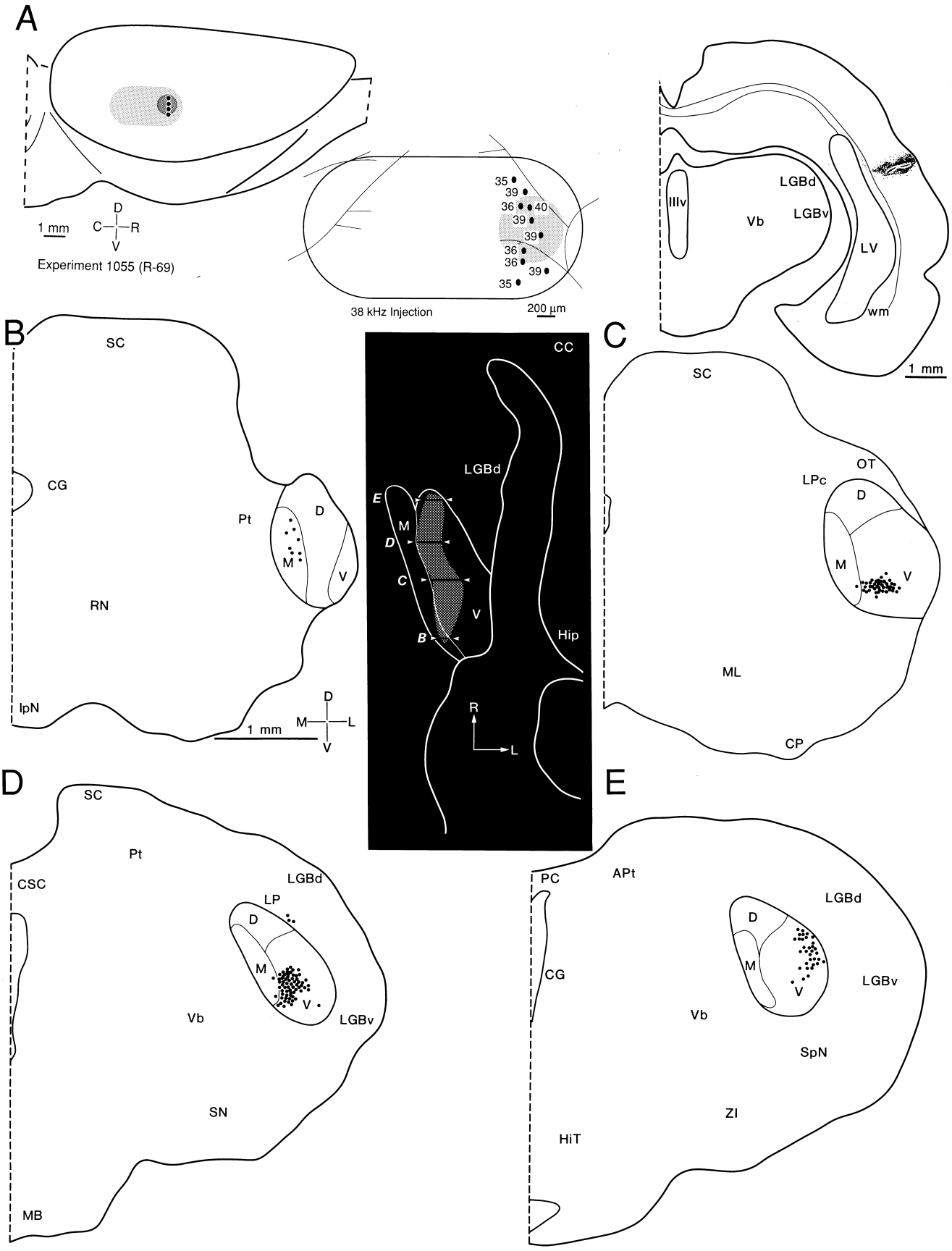
A
1 mm
D
C
R
V
Experiment 1055 (R-69)
35
39
36
40
39
39
36
36
39
35
38 kHz Injection
200 µm
IIIv
LGBd
Vb
LGBv
LV
wm
1 mm
B
SC
CG
Pt
D
M
V
RN
lpN
1 mm
D
M
L
V
CC
LGBd
E
M
D
C
V
B
Hip
R
L
C
SC
OT
LPc
D
M
V
ML
CP
D
SC
Pt
CSC
LGBd
LP
D
M
V
Vb
LGBv
SN
MB
E
PC
APt
LGBd
D
M
V
CG
LGBv
Vb
SpN
ZI
HiT

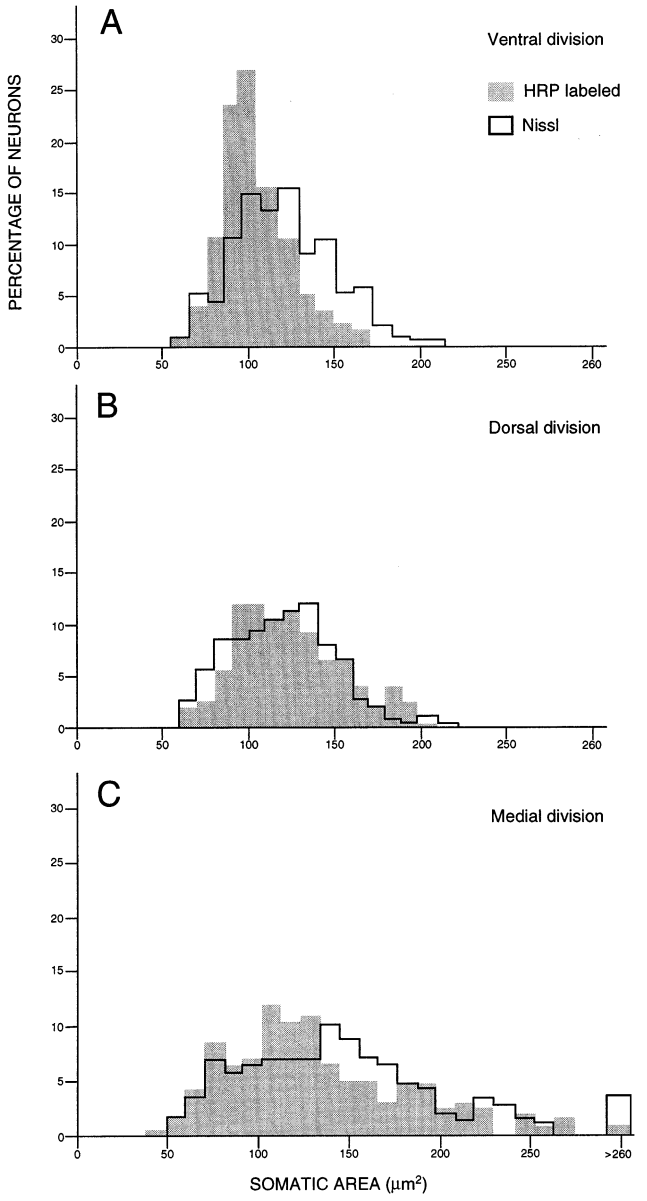

Fig. 7. Somatic size profiles of neurons retrogradely labeled with horseradish peroxidase (stippled) or Nissl stained (black line) compared in the three medial geniculate divisions. One hundred of each type of neuron were measured for each histogram. The average size and standard deviations within each histogram were indistinguishable, and the neuronal populations were normally distributed and unimodal. The degree of overlap in the histograms suggests that almost all medial geniculate body neurons project to the neocortex (Winer and Larue, 1987, 1988 [rat]). A: Ventral division. B: Dorsal division. C: Medial division. The range of this distribution implies that more than one type of projection neuron might be present.

est, 1964, 1965, 1971, 1975), which is reduced concomitantly in the rat.

The last constraint is the spatial distribution and structure of thalamocortical axons. Retrograde methods can provide only indirect estimates of the total dorso-ventral limits of any isofrequency band, and they are even less informative about precise values for the terminal distribution of single axons. In the cat, small injections of different tracers into discrete portions of a physiologically defined cortical isofrequency contour tend to single-label adjoining or segregated clusters of auditory thalamic cells of origin (Brandner and Redies, 1990). The study referred to noted that the exceptions to a point-to-point representation were most pronounced in more rostral sections, an observation consistent with the present outcome and which suggests that even topographies which may in principle seem simple are, in fact, marked by local discontinuities. This suggests that gradients or complexities in the internal configuration of thalamic isofrequency laminae exist whose significance remains to be explored in experimental work.

4.3. Revisiting the idea of parallel thalamocortical pathways

Since about 1970, one of the most influential concepts in central sensory processing has been that the output from single receptors is represented centrally through progressive connectional divergence, which leads to many topographic maps of the periphery in a variety of species (Woolsey, 1982; Dykes, 1983; Stone, 1983). The anatomical substrate for this process at the level of the auditory thalamus and cortex was the result from experimental tract tracing studies in which lesions to different thalamic nuclei resulted in lamina-specific degeneration, with the ventral division projecting to layers III and IV and the medial division to layers I and VI (Killackey and Ebner, 1972 [opossum and hedgehog]).

Subsequent work has enlarged the concept of parallel representation to the point where it is now possible to compare and contrast the different streams of afferent information across dimensions other than connectivity alone. The ensuing, contemporary picture (Table 1) enlarges and clarifies the earlier view, as some examples show, and it can suggest new levels of complexity that

→

Fig. 8. Photomicrographs of three characteristic patterns of retrograde labeling in the auditory thalamus after tracer injections in primary and nonprimary auditory cortex. A: After an injection that saturated areas 41, 20, and 36, every auditory thalamic divisions had many labeled neurons (see Fig. 9, and Winer and Larue, 1987 [rat]). Protocol for all panels: wheat germ agglutinin conjugated to horseradish peroxidase and reacted with diaminobenzidine as the chromogen; 60 μm thick frozen sections. Planapochromat, N.A. 0.16, ×62. B: Labeling after deposits caudal to area 41. Retrograde labeling was concentrated in the dorsal division nuclei and the marginal zone. C: In a third experiment, an auditory cortex injection labeled medial division neurons through its caudo-rostral extent. Other neurons were labeled in the ventral (V), and dorsal (D) divisions, as well as in the nearby tegmentum (LMN).

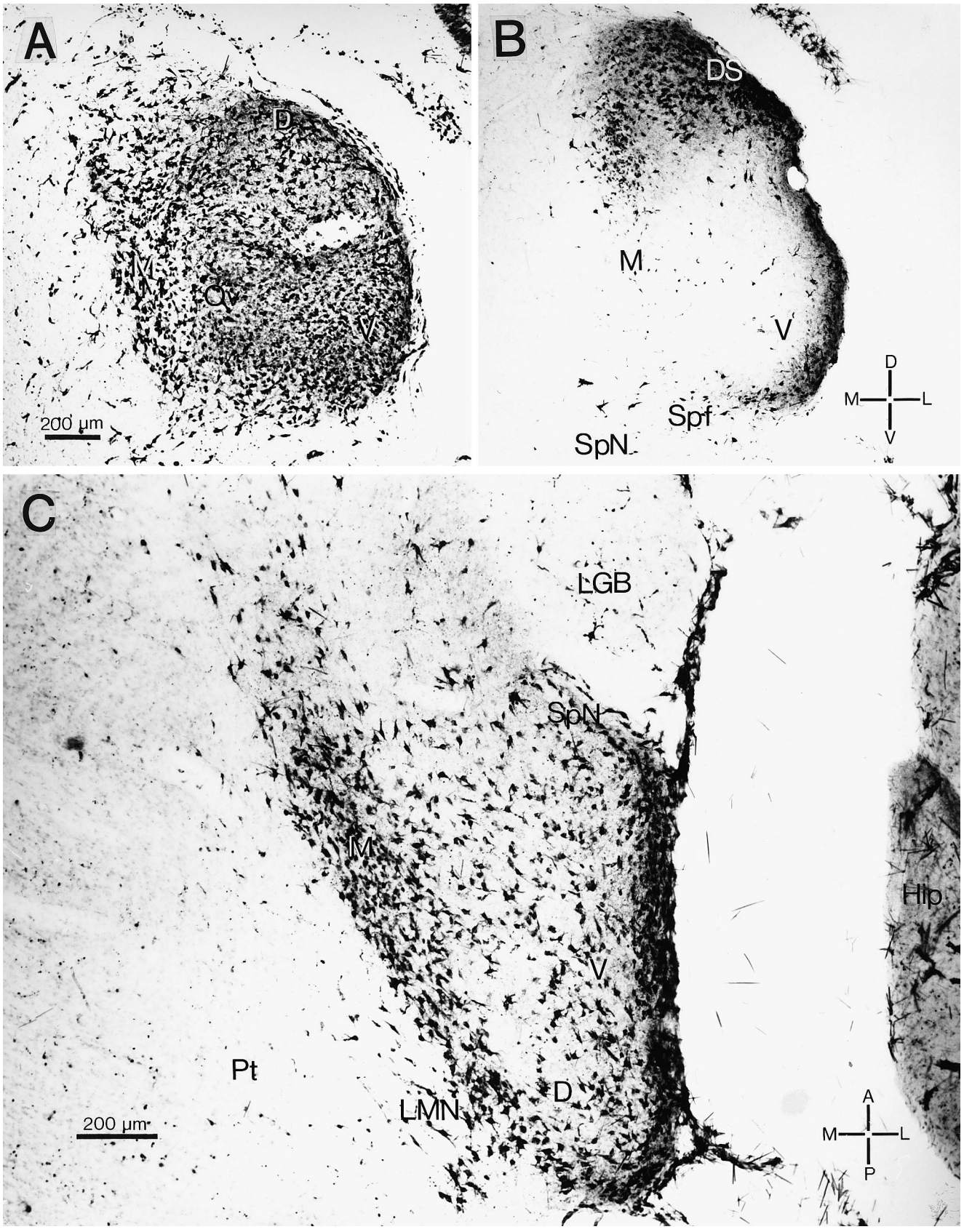
A
D
M
CV
V
200 μm
B
DS
M
V
Spf
SpN
D
M
L
V
C
LGB
SpN
M
V
Pt
D
LMN
Hip
200 μm
A
M
L
P

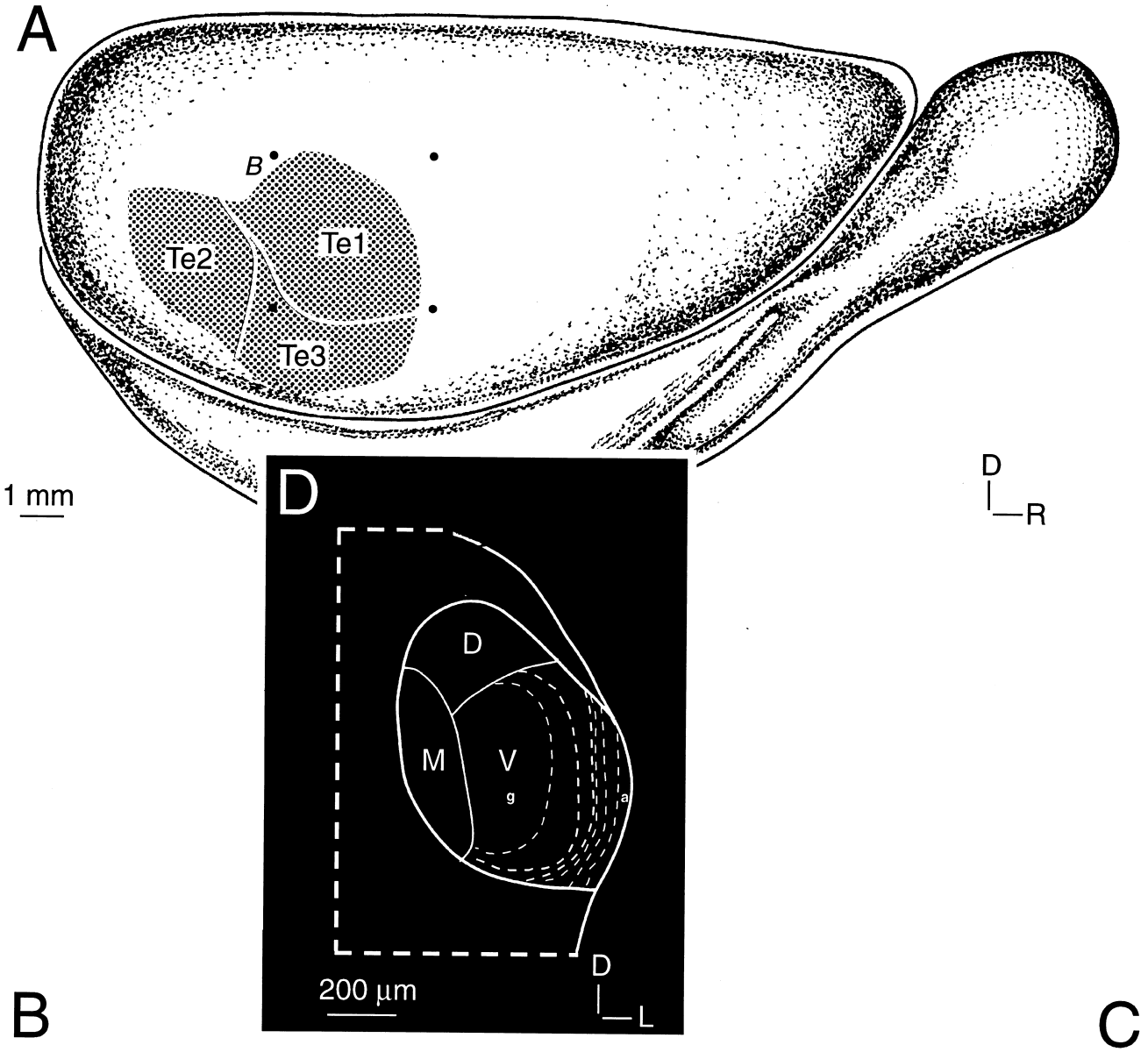
A
B
Te2
Te1
Te3
1 mm
D
R
D
D
M
V
g
a
200 μm
D
L
B
C
NR
6.8
.95
5.5
20.8
.80
1.5
5.0
9.0
30.5
38.0
40.2
44.0
.93
14.5
20.8
21.0
23.6
33.0
40.3
40.1
44.6
41.1
1.8
14.3
19.0
24.
16.7
18.2
25.3
32.3
36.0
35.0
1.9
12.5
17.4
29.
33.6
33.3
37.0
.45
3.5
15.7
22.2
33.5
35.0
1.6
13.7
15.3
27.5
32.4
33.4
12.8
20.5
3.8
10.6
13.3
28.4
32.0
.75
5.3
12.1
20.2
25.3
30.4
8.3
13.0
33.0
D
R
1 mm
0
1
2
3
4
a
b
c
d
e
f
g

Fig. 9. Hypothetical representation of best frequency in the rat medial geniculate body derived from isofrequency representation in auditory cortex. A: Lateral view of cerebral hemisphere, onto which the principal auditory cytoarchitectonic fields (Te1–3) derived from other investigations (Zilles et al., 1990 [rat]) have been superimposed. B: Representation of unit best frequencies in albino rat primary auditory cortex in a typical experiment (for locus, see the boxed area in panel A) taken from mapping studies (Sally and Kelly, 1988 [rat]). There is a systematic representation from low (left side) to high (right side) frequencies organized along the caudo-rostral axis. Solid lines, major blood vessels; dashed lines, architectonic borders. C: Estimates of predicted octave boundaries taken from panel B and proceeding from low (a) to high (g) frequency. D: Schematic view of postulated isofrequency contours in the ventral division of the rat medial geniculate body. This was constructed by computing the area under each octave value in panel C and adjusting the shape of each isofrequency contour to match that of the fibrodendritic laminae represented in Golgi preparations (Winer et al., 1999 [rat]).
←

remain to be described more fully. Consider the dimension of modality (Table 1), in which the so-called primary pathway is exclusively auditory and the nonprimary pathway is construed as polymodal. In fact, the exclusively auditory cortex receives many different, chemically specific and probably extra-auditory inputs, including serotoninergic (DeFelipe et al., 1991 [cat]), dopaminergic (Campbell et al., 1987 [monkey]) and cholinergic (Aoki and Kabak, 1992 [cat]) afferents, to name just a few. It might be argued that these are common denominators of sensory cortex (McCormick, 1992) and hardly unique to primary auditory cortex. Since there is cholinergic (Edeline et al., 1994a,b [rat]) and adrenergic (Edeline, 1995 [rat]) modulation of forebrain auditory neurons, these chemically diverse subsystems may be distributed widely. Nonetheless, they act directly and specifically on auditory neurons. One possible role for the cholinergic auditory neocortical innervation is to facilitate rapid changes in the representation of frequency, suggesting that the map of best frequency may be more plastic from a functional perspective than the topography of thalamocortical connectivity might seem to imply (Weinberger, 1997; Kilgard and Merzenich, 1998 [rat]). In any event, it suggests a prospectively dynamic role in cortex for extrathalamic input whose roles might have once been regarded as ancillary to the dominant thalamocortical projection.

The tuning curves of cat cortical neurons provide another pertinent example of the physiological complexity that seems to confound simplistically dichotomous functional categories. Even in AI, cells having multipeaked tuning curves with a broad range of tonal bandwidths and elaborate inhibitory/suppressive sidebands are intermingled with single-peaked neurons (Sutter and Schreiner, 1991 [cat]). If such neurons exist in the rat, they could signify a kind of spectrotemporal combination sensitivity, which suggests either that an area often considered as functionally homogeneous previously in fact contains subregions, or that some part of it receives specific input with unique intrinsic function. It also implies that descriptors of nuclei and areas in the thalamocortical auditory system underestimate the computational power of tightly coupled ensembles of neurons (Lund et al., 1995 [monkey]).

Acknowledgments

We are grateful to Ms. Pamela Woronoff for assistance with Figures 7 and 9. Supported by a United States Public Health Service grant (R01 DC 02319-19; J.A.W.) and by a Natural Sciences and Engineering Research Council of Canada grant (J.B.K.).

References

Aitkin, L.M., 1973. Medial geniculate body of the cat: responses to tonal stimuli of neurons in medial division. J. Neurophysiol. 36, 275–283.

Aitkin, L.M., 1990. The Auditory Cortex: Structural and Functional Bases of Auditory Perception. Chapman and Hall, London.

Aitkin, L.M., Webster, W.R., 1972. Medial geniculate body of the cat: organization and responses to tonal stimuli of neurons in ventral division. J. Neurophysiol. 35, 365–380.

Aoki, C., Kabak, S., 1992. Cholinergic terminals in the cat visual cortex: ultrastructural basis for interaction with glutamate-immunoreactive neurons and other cells. Vis. Neurosci. 8, 177–191.

Arnault, P., Roger, M., 1990. Ventral temporal cortex in the rat: connections of secondary auditory areas Te2 and Te3. J. Comp. Neurol. 302, 110–123.

Brandner, S., Redies, H., 1990. The projection of the medial geniculate body to field AI: organization in the isofrequency dimension. J. Neurosci. 10, 50–61.

Burwell, R.D., Witter, M.P., Amaral, D.G., 1995. Perirhinal and postrhinal cortices of the rat: a review of the neuroanatomical literature and comparison with findings from the monkey brain. Hippocampus 5, 390–408.

Calford, M.B., 1983. The parcellation of the medial geniculate body of the cat defined by the auditory response properties of single units. J. Neurosci. 3, 2350–2364.

Calford, M.B., Webster, W.R., 1981. Auditory representation within principal division of cat medial geniculate body: an electrophysiological study. J. Neurophysiol. 45, 1013–1028.

Campbell, M.J., Lewis, D.A., Foote, S.L., Morrison, J.H., 1987. Distribution of choline acetyltransferase-, serotonin-, dopamine-β-hydroxylase-, tyrosine hydroxylase-immunoreactive fibers in monkey primary auditory cortex. J. Comp. Neurol. 261, 209–220.

Clarey, J.C., Barone, P., Imig, T.J., 1992. Physiology of thalamus and cortex. In: Popper, A.N., Fay, R.R. (Eds.), Springer Handbook of Auditory Research, Vol. 2, The Mammalian Auditory Pathway: Neurophysiology. Springer-Verlag, New York, pp. 232–334.

Clerici, W.J., Coleman, J.R., 1990. Anatomy of the rat medial geniculate body: I. Cytoarchitecture, myeloarchitecture, and neocortical connectivity. J. Comp. Neurol. 297, 14–31.

Clerici, W.J., McDonald, A.J., Thompson, R., Coleman, J.R., 1990. Anatomy of the rat medial geniculate body: II. Dendritic morphology. J. Comp. Neurol. 297, 32–54.

Deacon, T.W., Eichenbaum, H., Rosenberg, P., Eckmann, K.W., 1983. Afferent connections of the perirhinal cortex in the rat. J. Comp. Neurol. 220, 168–190.

DeFelipe, J., Hendry, S.H.C., Hashikawa, T., Jones, E.G., 1991. Synaptic relationships of serotonin immunoreactive terminal baskets on GABA neurons in the cat auditory cortex. Cereb. Cortex 1, 117–133.

Diamond, M.E., Armstrong-James, M., Budway, M.J., Ebner, F.F., 1992. Somatic sensory responses in the rostral sector of the posterior group (POm) and in the ventral posterior medial nucleus (VPM) of the rat thalamus: dependence on the barrel field cortex. J. Comp. Neurol. 319, 66–84.

Dykes, R.W., 1983. Parallel processing of somatosensory information: a theory. Brain Res. Rev. 6, 47–115.

Edeline, J.-M., 1995. The α2-adrenergic antagonist idazoxan enhances the frequency selectivity and increases the threshold of auditory cortex neurons. Exp. Brain Res. 107, 221–240.

Edeline, J.-M., Hars, B., Maho, C., Hennevin, E., 1994a. Transient and prolonged facilitation of tone-evoked responses induced by basal forebrain stimulations in the rat auditory cortex. Exp. Brain Res. 97, 373–386.

Edeline, J.-M., Maho, C., Hars, B., Hennevin, E., 1994b. Non-awaking basal forebrain stimulation enhances auditory cortex responsiveness during slow-wave sleep. Brain Res. 636, 333–337.

Games, K.D., Winer, J.A., 1988. Layer V in rat auditory cortex: projections to the inferior colliculus and contralateral cortex. Hear. Res. 34, 1–26.

Gerren, R.A., Weinberger, N.M., 1983. Long term potentiation in the magnocellular medial geniculate nucleus of the anesthetized cat. Brain Res. 265, 138–142.

Glassman, R.B., Forgus, M.W., Goodman, J.E., Glassman, H.N., 1975. Somesthetic effects of damage to cats' ventrobasal complex, medial lemniscus or posterior group. Exp. Neurol. 48, 460–492.

Harris, R.M., 1987. Axon collaterals in the thalamic reticular nucleus from thalamocortical neurons of the rat ventrobasal complex. J. Comp. Neurol. 258, 397–406.

Hashikawa, T., Molinari, M., Rausell, E., Jones, E.G., 1995. Patchy and laminar terminations of medial geniculate axons in monkey auditory cortex. J. Comp. Neurol. 362, 195–208.

Hindmarsh, J.L., Rose, R.M., 1994. A model of intrinsic and driven spindling in thalamocortical neurons. Phil. Trans. R. Soc. Lond. B 346, 165–183.

Huang, C.L., Winer, J.A., 1997. Areal and laminar distribution of cat auditory thalamocortical projections. Proc. Soc. Neurosci. 24, 185.

Imig, T.J., Morel, A., 1985. Tonotopic organization in ventral nucleus of medial geniculate body in the cat. J. Neurophysiol. 53, 309–340.

Jones, E.G., Burton, H., 1976. Areal differences in the laminar distribution of thalamic afferents in cortical fields of the insular, parietal, and temporal regions of primates. J. Comp. Neurol. 168, 197–248.

Kelly, J.B., 1990. Rat auditory cortex. In: Kolb, B., Tees, R.C. (Eds.), The Cerebral Cortex of the Rat. MIT Press, Cambridge, MA, pp. 380–405.

Kelly, J.B., Judge, P.W., 1985. Effects of medial geniculate lesions on sound localization by the rat. J. Neurophysiol. 53, 361–372.

Kilgard, M.P., Merzenich, M.M., 1998. Cortical map reorganization enabled by nucleus basalis activity. Science 279, 1714–1718.

Killackey, H.P., Ebner, F.F., 1972. Two different types of thalamocortical projections to a single cortical area in mammals. Brain Behav. Evol. 6, 141–169.

LeDoux, J.E., Farb, C.R., 1991. Neurons of the acoustic thalamus that project to the amygdala contain glutamate. Neurosci. Lett. 134, 145–149.

LeDoux, J.E., Ruggiero, D.A., Reis, D.J., 1985. Projections to the subcortical forebrain from anatomically defined regions of the medial geniculate body in the rat. J. Comp. Neurol. 242, 182–213.

Lund, J.S., Wu, Q., Hadingham, P.T., Levitt, J.B., 1995. Cells and circuits contributing to functional properties in area V1 of macaque monkey cerebral cortex: bases for neuroanatomically realistic models. J. Anat. (Lond.) 187, 563–581.

McCormick, D.A., 1992. Neurotransmitter actions in the thalamus and cerebral cortex and their role in neuromodulation of thalamocortical activity. Prog. Neurobiol. 39, 337–388.

McCormick, D.A., von Krosigk, M., 1992. Corticothalamic activation modulates thalamic firing through glutamate 'metabotropic' receptors. Proc. Natl. Acad. Sci. USA 89, 2774–2778.

Mesulam, M.-M., 1978. Tetramethyl benzidine for horseradish peroxidase neurohistochemistry: a non-carcinogenic blue reaction-product with superior sensitivity for visualizing neural afferents and efferents. J. Histochem. Cytochem. 26, 106–117.

Middlebrooks, J.C., Zook, J.M., 1983. Intrinsic organization of the cat's medial geniculate body identified by projections to binaural response-specific bands in the primary auditory cortex. J. Neurosci. 3, 203–225.

Morest, D.K., 1964. The neuronal architecture of the medial geniculate body of the cat. J. Anat. (Lond.) 98, 611–630.

Morest, D.K., 1965. The laminar structure of the medial geniculate body of the cat. J. Anat. (Lond.) 99, 143–160.

Morest, D.K., 1971. Dendrodendritic synapses of cells that have axons: the fine structure of the Golgi type II cell in the medial geniculate body of the cat. Z. Anat. Entwicklungsgesch. 133, 216–246.

Morest, D.K., 1975. Synaptic relations of Golgi type II cells in the medial geniculate body of the cat. J. Comp. Neurol. 162, 157–194.

Niimi, K., Naito, F., 1974. Cortical projections of the medial geniculate body in the cat. Exp. Brain Res. 19, 326–342.

Patterson, H.A., 1976. An Anterograde Degeneration and Retrograde Axonal Transport Study of the Cortical Projections of the Rat Medial Geniculate Body. Ph.D. Thesis, Department of Anatomy, Boston University Graduate School, Boston, MA.

Popowits, J.M., Larue, D.T., Winer, J.A., 1988. Glutamate is a major transmitter in the rat medial geniculate body. Proc. Soc. Neurosci. 14, 490.

Reale, R.A., Imig, T.J., 1980. Tonotopic organization in auditory cortex of the cat. J. Comp. Neurol. 182, 265–291.

Romanski, L.M., LeDoux, J.E., 1993a. Information cascade from primary auditory cortex to the amygdala: corticocortical and corticoamygdaloid projections of temporal cortex in the rat. Cereb. Cortex 3, 515–532.

Romanski, L.M., LeDoux, J.E., 1993b. Organization of rodent auditory cortex: anterograde transport of PHA-L from MGv to temporal neocortex. Cereb. Cortex 3, 499–514.

Rouiller, E.M., Rodrigues-Dagaeff, C., Simm, G., de Ribaupierre, Y., Villa, A., de Ribaupierre, F., 1989. Functional organization of the medial division of the medial geniculate body of the cat: tonotopic organization, spatial distribution of response properties and cortical connections. Hear. Res. 39, 127–146.

Ryugo, D.K., Killackey, H.P., 1974. Differential telencephalic projections of the medial and ventral divisions of the medial geniculate body of the rat. Brain Res. 82, 173–177.

Sally, S.L., Kelly, J.B., 1988. Organization of auditory cortex in the albino rat: sound frequency. J. Neurophysiol. 59, 1627–1638.

Schreiner, C.E., 1992. Functional organization of the auditory cortex: maps and mechanisms. Curr. Opin. Neurobiol. 2, 516–521.

Shinonaga, Y., Takada, M., Mizuno, N., 1994. Direct projections from the non-laminated divisions of the medial geniculate nucleus to the temporal polar cortex and amygdala in the cat. J. Comp. Neurol. 340, 405–426.

Smith, Y., Séguéla, P., Parent, A., 1987. Distribution of GABA-immunoreactive neurons in the thalamus of the squirrel monkey (*Saimiri sciureus*). Neuroscience 22, 579–591.

Sousa-Pinto, A., 1973. Cortical projections of the medial geniculate body in the cat. Adv. Anat. Embryol. Cell Biol. 48, 1–42.

Stone, J., 1983. Parallel Processing in the Visual System. The Classification of Retinal Ganglion Cells and Its Impact on the Neurobiology of Vision. Plenum Press, New York.

Sun, X., Chen, Q.C., Jen, P.H.-S., 1996. Corticofugal control of central auditory sensitivity in the big brown bat, *Eptesicus fuscus*. Neurosci. Lett. 212, 131–134.

Sutter, M.L., Schreiner, C.E., 1991. Physiology and topography of neurons with multipeaked tuning curves in cat primary auditory cortex. J. Neurophysiol. 65, 1207–1226.

Vaughan, D.W., 1983. Thalamic and callosal connections of the rat auditory cortex. Brain Res. 260, 181–189.

Weinberger, N.M., 1997. Learning-induced receptive field plasticity in the auditory cortex. Semin. Neurosci. 9, 59–67.

Weinberger, N.M., Diamond, D.M., 1987. Physiological plasticity in auditory cortex: rapid induction by learning. Prog. Neurobiol. 29, 1–55.

Wepsic, J.G., 1966. Multimodal sensory activation of cells in the magnocellular medial geniculate nucleus. Exp. Neurol. 15, 299–318.

Winer, J.A., Larue, D.T., 1987. Patterns of reciprocity in auditory thalamocortical and corticothalamic connections: study with horseradish peroxidase and autoradiographic methods in the rat medial geniculate body. J. Comp. Neurol. 257, 282–315.

Winer, J.A., Larue, D.T., 1988. Anatomy of glutamic acid decarboxylase (GAD) immunoreactive neurons and axons in the rat medial geniculate body. J. Comp. Neurol. 278, 47–68.

Winer, J.A., Larue, D.T., 1996. Evolution of GABAergic circuitry in the mammalian medial geniculate body. Proc. Natl. Acad. Sci. USA 93, 3083–3087.

Winer, J.A., Morest, D.K., 1983a. The medial division of the medial geniculate body of the cat: implications for thalamic organization. J. Neurosci. 3, 2629–2651.

Winer, J.A., Morest, D.K., 1983b. The neuronal architecture of the dorsal division of the medial geniculate body of the cat. A study with the rapid Golgi method. J. Comp. Neurol. 221, 1–30.

Winer, J.A., Morest, D.K., 1984. Axons of the dorsal division of the medial geniculate body of the cat: a study with the rapid Golgi method. J. Comp. Neurol. 224, 344–370.

Winer, J.A., Kelly, J.B., Larue, D.T. (1999) Neural architecture of the rat medial geniculate body. Hear. Res. (in press).

Woolsey, C.N. (Ed.) (1982) Cortical Sensory Organization, Vol. 3, Multiple Auditory Areas. Humana Press, Clifton, NJ.

Zilles, K., Wree, A., Dausch, N.-D., 1990. Anatomy of the neocortex: neurochemical organization. In: Kolb, B., Tees, R.C. (Eds.), The Cerebral Cortex of the Rat. MIT Press, Cambridge, MA, pp. 113–150.